

$^{140}\text{Ce}(d,p)^{141}\text{Ce}$ at 17 MeV†

J. E. Park, W. W. Daehnick, and M. J. Spisak

Nuclear Physics Laboratory, University of Pittsburgh, Pittsburgh, Pennsylvania 15260

(Received 27 September 1976)

The reaction $^{140}\text{Ce}(d,p)$ has been studied at an incident deuteron energy of 17 MeV. Reaction protons were detected with an Enge split-pole spectrograph using a high-resolution position-sensitive (helix) gas counter and photographic emulsions as detectors. The energy resolution ranged from 11 to 13 keV. Angular distributions were measured in 3–5° steps for $6^\circ \leq \theta \leq 55^\circ$. l -transfer assignments and spectroscopic factors have been deduced for 46 levels up to an excitation energy of 3.7 MeV in ^{141}Ce by comparison with zero-range distorted-wave Born approximation calculations. We note that in spite of the neutron shell closure at $N = 82$, no ^{141}Ce state has a spectroscopic factor in excess of 0.80. All neutron states are fragmented and considerable spectroscopic strength for $l = 1$ and 3 is spread up to and above 3 MeV. Two well resolved fragments each for the $h_{9/2}$ and $i_{13/2}$ states very nearly fill the sum rules for these single-particle states. The structure of ^{141}Ce levels below 2 MeV is well reproduced by the unified model calculations of Heyde, Waroquier, and Vincx.

[NUCLEAR REACTIONS $^{140}\text{Ce}(d,p)$, $E_d = 17$ MeV; measured $\sigma(E_p, \theta)$, resolution 11 keV. DWBA analysis, deduced l , π , J , spectroscopic factors.]

I. INTRODUCTION

Neutron transfer by (d,p) stripping on $^{140}\text{Ce}_{82}$ provides important information on single-particle states in the 82–126 neutron shell. Earlier investigations of this reaction^{1–3} and other studies of the level scheme of ^{141}Ce , by $^{140}\text{Ce}(n,\gamma)$ (Ref. 4), pickup reactions (Refs. 5 and 6), β decay of ^{141}La (Ref. 7), and isobaric analog resonances (Ref. 8) as compiled by Auble⁹ gave contradictory information regarding ^{141}Ce J^π assignments and spectroscopic factors.

Since apparent contradictions may be caused by unresolved doublets, we have reexamined the $^{140}\text{Ce}(d,p)$ reaction at $E_d = 17$ MeV up to 3.7 MeV in ^{141}Ce with high energy resolution. We also explore the problem of missing spectroscopic strengths for $l = 1$ and 3 transitions and identifying the $l = 5$ and 6 states with their correct spectro-

scopic factors.

We shall compare our results with another recent study of the (d,p) reaction¹⁰ which was reported during the course of our analysis.

II. EXPERIMENTAL PROCEDURE

The experiment was carried out with a 17 MeV deuteron beam from the University of Pittsburgh three-stage Van de Graaff accelerator. The beam handling system and scattering chamber have been described in detail in Refs. 11 and 12. The scattered protons were detected by a high resolution position sensitive (helix) gas proportional counter¹³ and also with Kodak NTB 50 μm nuclear emulsions in the focal plane of an Enge split-pole spectrograph. Angular distributions for proton groups were taken at 17 angles between 6° and 55° , twice with helix counter and once with nuclear emulsions

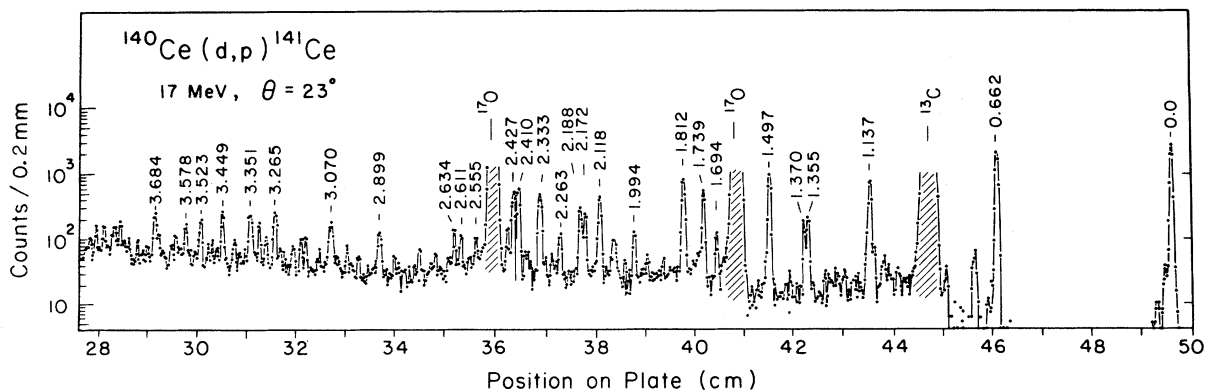


FIG. 1. Semilog graph of $^{140}\text{Ce}(d,p)^{141}\text{Ce}$ proton spectrum obtained with photographic emulsions. The resolution of 11 keV was caused primarily by target nonuniformity. Shaded areas indicate strong impurity peaks.

so that we were able to distinguish the rather unstructured $l=1$ and 3 angular distributions. The photographic emulsions were scanned in steps of 0.2 mm. Typical targets consisted of $\sim 90 \mu\text{g}/\text{cm}^2$ CeO on a $20 \mu\text{g}/\text{cm}^2$ carbon backing. Target thickness was measured by comparing elastic scattering of 17 MeV deuterons at small angles

with optical-model predictions. Charge collection and measurements of elastically scattered deuterons by NaI(Tl) scintillators at $\pm 38^\circ$ relative to the beam direction were used to monitor beam and target. A typical reaction spectrum is shown in Fig. 1. Major impurities are oxygen and carbon. Small amounts of tantalum, sodium, and silicone

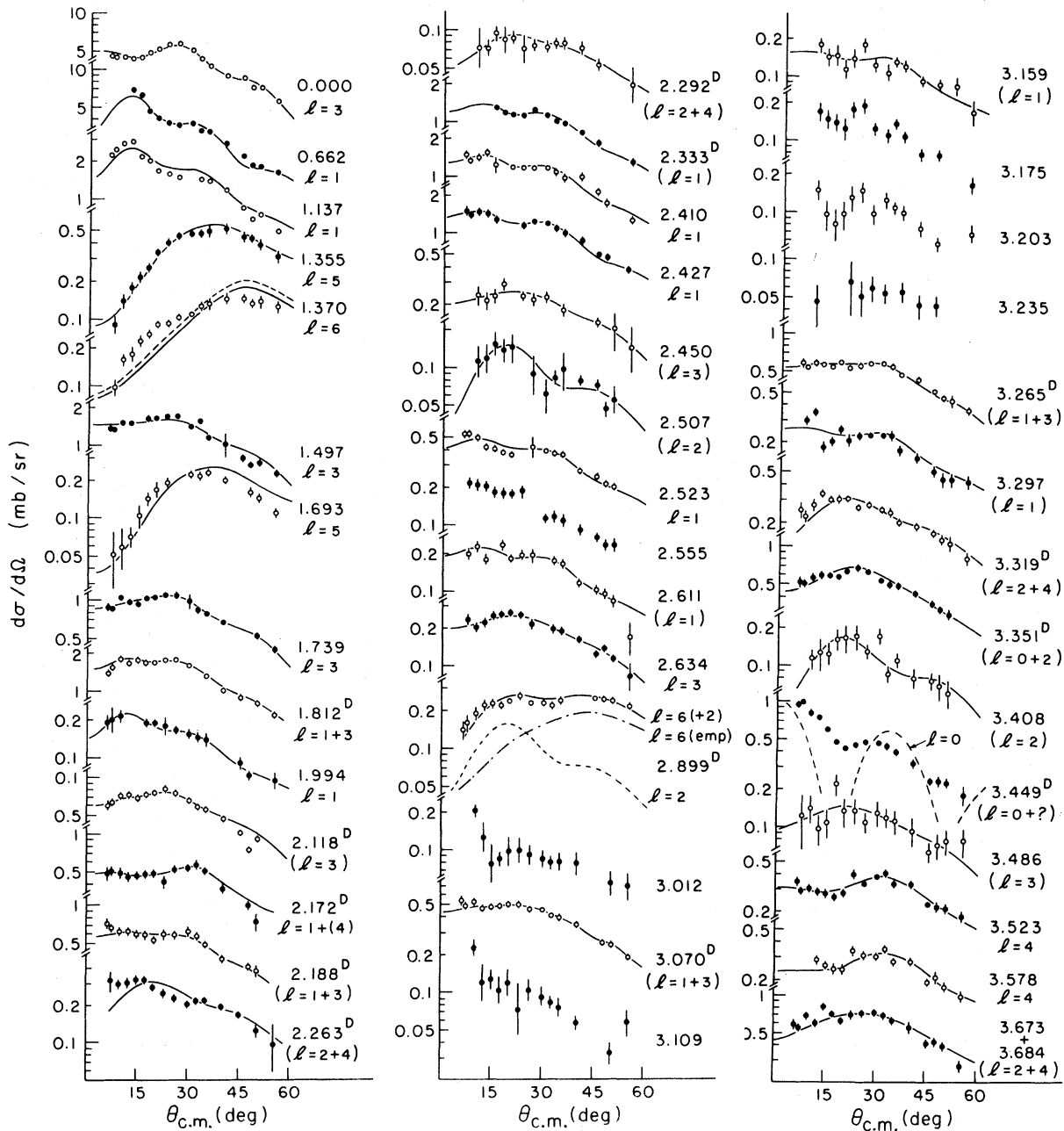


FIG. 2. Experimental $^{140}\text{Ce}(d,p)$ angular distributions compared with zero-range DWBA calculations and ordered by excitation energy. l values in brackets are tentative assignments. Unresolved, closely spaced doublets are indicated by the superscript D. Error bars contain all known and estimated random errors. Large errors are usually caused by uncertainties in separating close doublets or impurity peaks. Data without DWBA curves did not discriminate adequately between various l shapes.

were also present. The final level energy calibration was made by a direct comparison¹⁴ with five of the well-known states⁷ of ^{141}Ce .

The excitation-energy assignments, listed in Table II are believed to be accurate to within ± 2 keV below 3 MeV, and to ± 3 keV above 3 MeV in ^{141}Ce . The random monitoring error was $\leq 5\%$. It is the dominant error for the strong groups. Cross section errors for weak states are mainly due to statistics and include an estimate of errors in background subtraction and in separating doublets. We estimate the uncertainty in the absolute cross sections as $\pm 10\%$, because of systematic errors possible in determining target thickness and the spectrograph solid angle.

III. ANALYSIS AND RESULTS

The experimental angular distributions (shown in Fig. 2) were compared with distorted-wave Born approximation (DWBA) calculations made with code DWUCK.¹⁵ The finite range correction parameter used was 0.62 and the nonlocality parameters were $\beta_d = 0.54$ and $\beta_p = 0.85$. Nonlocality corrections were not made for the bound-state wave functions. These corrections had little effect on the predicted cross sections.

Deuteron optical-model parameters were taken from a global fit for 17 MeV deuterons¹⁶ and proton parameters from Becchetti and Greenlees.¹⁷ All optical-model parameters used are listed in Table I. DWBA calculations agreed well with our data except for the small angle behavior for $l=6$.

Spectroscopic factors were obtained by normalizing the DWBA predictions to the experimental angular distributions. Shell-model arguments are used for $l=5$ and 6 transfers which are expected to be $h_{9/2}$ and $i_{13/2}$, respectively. Deduced l and J^π values and spectroscopic strengths $(2J+1)S$ are listed in Table II. The recent data of Booth, Wilson, and Ipson¹⁰ and previously adopted levels of ^{141}Ce are included in Table II for the purpose of comparison.

IV. DISCUSSION

Inspection of Figs. 1 and 3 reveals features somewhat unexpected for a closed shell target.

Instead of finding six dominant states corresponding to the six single-particle states of the 82–126 shell, we see about twice as many strong states—all belonging to this shell—as well as a large number of weaker levels. In addition there are a number of reasonably strong states above 3.3 MeV which apparently contain fractions of single-particle strengths of the $N > 126$ shell. Figure 3 shows the measured distribution of spectroscopic strengths in a quantitative way. Only the $\frac{7}{2}^-$ ground state of ^{141}Ce has a reasonably pure (79%) single-particle configuration. Other single-particle strengths are split into two or more significant pieces. The $l=1$ strength shows a particularly suggestive behavior. 40% of the total $l=1$ strength is found near 1 MeV, about 40% is clustered near 2.4 MeV, and the rest apparently remains undetected at excitations above 3.5 MeV. Similarly dramatic is the 1.5 MeV splitting of the two detected pieces of $i_{13/2}$ strength.

This fractionation of the single-particle strengths has been found in other $N=83$ nuclei as well^{10,19} and has been attributed to a strong mixing of single-particle states with weak-coupling states of quadrupole and octupole core excitations.^{10,18,19} Heyde, Waroquier, and Vincx¹⁸ have performed unified model calculations for $N=83$ nuclei and—using properties of low-lying ^{140}Ce and ^{141}Ce states—make specific predictions for the structure of higher-lying ^{141}Ce levels, which will be compared with results of the present study.

Early studies of $^{140}\text{Ce}(d,p)$ at much lower energies or with poorer resolution¹⁻³ are largely superseded by the recent work of Booth, Wilson, and Ipson at 19 MeV.¹⁰ The present work improves on the study by Booth *et al.* in terms of better resolution (11 vs 18 keV), better statistics, and the inclusion of data at smaller angles. Hence we can often resolve and document doublets where they have been postulated or remained unnoticed in Ref. 10. In a few cases discussed below we disagree with Booth *et al.*, but generally good agreement is found as shown in Table II. There is a quantitative difference in $l=5$ and $l=6$ spectroscopic factors which at least in part is due to our use of a more diffuse neutron bound state potential

TABLE I. Optical-model parameters used in $^{140}\text{Ce}(d,p)^{141}\text{Ce}$ DWBA calculations.

	V (MeV)	r_0 (fm)	a_0 (fm)	W_D (MeV)	W_D (MeV)	r_I (fm)	a_I (fm)	V_{so} (MeV)	r_{so} (fm)	a_{so} (fm)
$d + ^{140}\text{Ce}$	105.60	1.10	0.82	0	15.9	1.25	0.81	5.63	0.98	1.0
$p + ^{141}\text{Ce}$	56.63	1.17	0.75	1.04	9.18	1.32	0.63	6.60	1.01	0.75
Bound neutron 1.	a	1.20	0.75					$\lambda = 25$		
2.	a	1.25	0.65					$\lambda = 25$		

^a Well depth adjusted by code to fit neutron separation energy.

TABLE II. Spectroscopic results for ^{141}Ce and comparison with previous work.

E_x (MeV)	Present work $E_d = 17$ MeV				Booth <i>et al.</i> (Ref. 10) $E_d = 19$ MeV			Nuclear Data Sheets (Ref. 9)	
	l	J^π	S	$(2J+1)S$	E_x (MeV)	l	$(2J+1)S$	E_x (MeV)	J^π
0	3	$\frac{7}{2}^-$	0.79	6.34	0	3	6.14	0	$\frac{7}{2}^-$
0.662	1	$\frac{3}{2}^-$	0.42	1.68	0.662	1	1.84	0.662 05	$\frac{3}{2}^-$
1.137	1	$(\frac{1}{2}^-)$	0.37	0.73	1.137	1	0.78	1.1370	$\frac{1}{2}^-, \frac{3}{2}^-$
								1.2431	
1.355	5	$\frac{9}{2}^-$	0.70	7.0	1.353	} 5	5.26	1.354 52	
1.370	6	$\frac{13}{2}^+$	0.64	9.0 ± 1	1.363		} 6	5.39	1.368 68
1.497	3	$(\frac{5}{2}^-)$	0.27	1.60	1.496	3	1.42	1.497 02	$\frac{5}{2}^-, \frac{7}{2}^-$
								1.6261	
1.693	5	$\frac{9}{2}^-$	0.29	2.91	1.692	5	2.17	1.693 31	
1.739	3			0.92	1.740	3	0.98	1.739 01	$\frac{5}{2}^-, \frac{7}{2}^-$
								1.780	$\frac{1}{2}^+$
1.812 ^a	} 1 } 3			0.23	1.810	} 1 } 3	0.38	1.8087	$(\frac{3}{2}^-)$
					0.92				0.71
								1.9438	
1.994	1			0.07	1.989	(1)	0.09	1.9940	
								2.030 19	
								2.0492	
2.118 ^a	(3)			0.58	2.123	3	0.61		
2.172 ^a	} 1 } (4)	$(\frac{3}{2}^+)$	0.04	0.09	2.177	} 3	0.40	2.1711	
							0.36		
2.188 ^a	} (1) } (3)			0.09	2.193	} 1	0.29	2.1896	$(\frac{1}{2}^-, \frac{3}{2}^-)$
					0.25				
2.209 ^b								2.2074	
								2.2269	
2.263 ^a	} (2) } (4)	$(\frac{9}{2}^+)$		0.05	2.271	Not assigned			
						0.12			
2.292 ^a	} (2) } (4)			0.01					
					0.06				
2.333 ^a	(1)			0.42	2.335	} 1 } 3	0.27	(2.3289)	
								0.19	2.3363
2.410	1			0.45	2.416	1	0.49	2.4108	$(\frac{1}{2}^-, \frac{3}{2}^-)$
2.427	1			0.45	2.429	} 1 } 3	0.18	2.4256	$(\frac{1}{2}^-, \frac{3}{2}^-)$
2.450	(3)			0.18				0.52	(2.440)
2.507	(2)			0.03					
2.523	1			0.14				2.5229	$(\frac{1}{2}^-, \frac{3}{2}^-)$
2.555	Not assigned								
2.611	(1)			0.07					
2.634	3			0.16					
2.899 ^a	} (2) } (6)	$\frac{13}{2}^+$	0.14	2.1 ± 0.2	2.906	6	3.15		
3.012	Not assigned								
3.070 ^a	} (1) } (3)			0.08	3.074	} 1 } 3	0.05		
					0.14				0.12
3.109	Not assigned								
3.159	(1)			0.05					
3.175	Not assigned								
3.203	Not assigned								
3.235	Not assigned								

TABLE II (Continued)

E_x (MeV)	Present work $E_d = 17$ MeV				Booth <i>et al.</i> (Ref. 10) $E_d = 19$ MeV			Nuclear Data Sheets (Ref. 9)	
	l	J^π	S	$(2J+1)S$	E_x (MeV)	l	$(2J+1)S$	E_x (MeV)	J^π
3.265 ^a	{ (1) (3)			0.11	3.272	1	0.32		
				0.17					
3.297	(1)			0.08					
3.319 ^a	{ (2) (4)			0.05					
				0.10					
3.351 ^a	{ 0 (2)	$\frac{1}{2}^+$	(0.02)	0.03	3.352	{ 1 3	0.08		
					0.14			0.26	
3.408	(2)			0.03					
3.449 ^a	(0+?)				3.450	1	0.26		
3.486	(3)			0.07					
3.523	(4)			0.34					
3.578	(4)			0.29					
3.673 ^c	[(2) (4)			0.06					
3.684 ^c				0.42					

^a Unresolved or poorly resolved doublet.

^b Weak state, only the excitation energy is measured.

^c The excitation energies were measured separately for these two close states at several angles.

(No. 1 in Table I) which has been found superior for transitions with poor angular momentum matching²⁰⁻²² and for heavy targets. The $r_0 = 1.2$ fm, $a_0 = 0.75$ fm well geometry is also favored by the global analysis of proton scattering.¹⁷ In order to facilitate a comparison with Ref. 10 we have made a second set of DWBA calculations using the "historical" bound well parameters $r_0 = 1.25$ fm and $a_0 = 0.65$ fm. As expected from earlier work there is no noteworthy difference for the two types of bound state wells for $l = 1$ and $l = 3$ predictions; however, our newer well shape predicts $l = 5$ cross sections 13% smaller and $l = 6$ cross sections 19% smaller than those obtained by the use of the historical geometry (bound state potential 2). Thus our spectroscopic factors would come closer to obeying the $h_{9/2}$ and $i_{13/2}$ sum rules than those of Ref. 10. Nevertheless, all $l = 6$ calculations remain a bit unsatisfactory as the cross sections below 30° are always poorly reproduced. We have assigned an explicit error of $\pm 10\%$ to $S_{13/2}$ to reflect the unavoidable arbitrariness of the relative normalization of data and calculations. (A quite similar shortcoming of DWBA shapes for $l = 6$ at 19 MeV can be observed in Fig. 5 of Ref. 10.)

Comparing our results with those of Ref. 10 we note the following experimental disagreements: Having resolved the 1.355 MeV ($\frac{9}{2}^-$), 1.370 MeV ($\frac{13}{2}^+$) doublet (see Fig. 1) we find the experimental cross sections for the $\frac{13}{2}^+$ state (and hence its spectroscopic factor) considerably larger than

assumed in Ref. 10. Even after allowing for differences in the DWBA treatment our extracted spectroscopic factors for the $\frac{9}{2}^-$ and $\frac{13}{2}^+$ states are 20 and 40% larger, respectively. In the region 2.17 to 2.19 MeV we find evidence for four levels; in Ref. 10 a single peak was seen and interpreted as only a doublet. Because of its unusual width and its atypical angular distribution we analyze the peak at 2.899 MeV as a doublet. This leads to a 33% lower $i_{13/2}$ strength for this high-lying fragment than given in Ref. 10. We present angular distributions for a fair number of states above 2.2 MeV which might have been seen in Ref. 10 but were not reported. Many of them are close doublets and of positive parity with angular distributions best fitted by $l = 2$ and 4. A disagreement exists for a doublet at 3.351 MeV. We need $l = 0 + 2$ contributions for acceptable fits whereas Ref. 10 suggests a doublet with $l = 1 + 3$.

Comparing our results with the latest Nuclear Data Sheets⁹ we find no disagreement with the adopted level energies or spin assignments. (See Table II.) However, we see no evidence at all for a level at 1.383 MeV supposed to have been observed in (d,p) . We agree with Ref. 10 that this assignment must be erroneous.

V. COMPARISON WITH THEORY

Figure 3 shows the summed spectroscopic strengths as well as their maximum values ex-

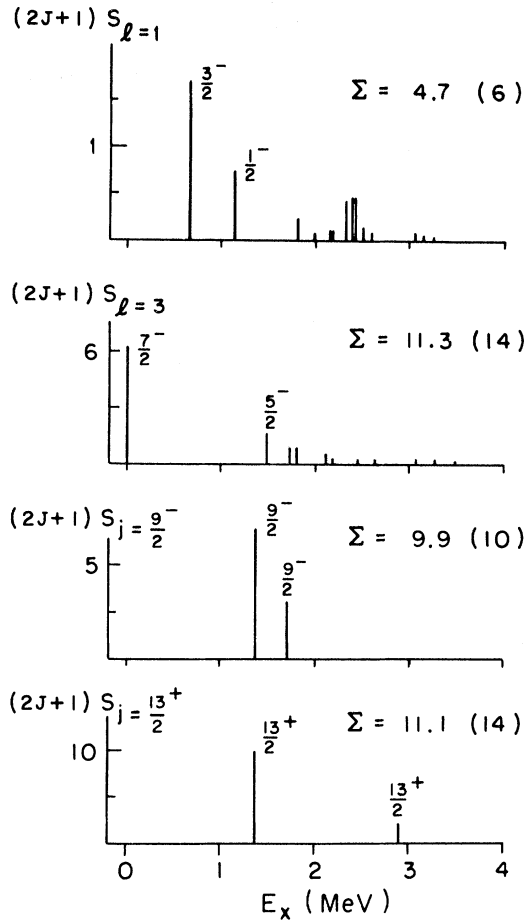


FIG. 3. Graphs of spectroscopic strengths for $^{140}\text{Ce}(d,p)^{141}\text{Ce}$. Averages of $p_{1/2}$ and $p_{3/2}$, or $f_{5/2}$ and $f_{7/2}$ DWBA calculations were used to extract strengths of peaks not otherwise identified. Note the extensive spreading of $l=1$ and $l=3$ strengths and some apparently missing strength for $l=1, 3$, and 6. Numbers in brackets are maximum $\Sigma(2J+1)S$ values from sum rules.

pected from the sum rules. We note that our analysis up to 3.5 MeV yields about 80% of all available single-particle strengths—save that for $h_{9/2}$ for which 99% seems to be found in the two lowest $\frac{9}{2}^-$ levels. This indicates that our DWBA and experimental normalizations fall closer to the correct value than one has a right to expect, and that comparisons with theory should be made without renormalizations. Heyde *et al.*¹⁸ have made available detailed results of their ^{141}Ce unified model calculation including the predicted spectroscopic factors for states up to 3.5 MeV. We note remarkably good agreement (within $\pm 15\%$) in S_j for almost all levels below 2 MeV, especially for the high spin states. From 2 to 3 MeV twice as many levels are observed as are predicted and correlations are difficult except for the second $\frac{13}{2}^+$ level, which is well reproduced. Finally, above 3 MeV the model seems to fail. The third $\frac{9}{2}^-$ and $\frac{13}{2}^+$ states are predicted to have spectroscopic factors of 0.12 and 0.16, respectively. No states even approaching such strengths have been found. Similarly absent is a strong predicted $f_{5/2}$ level near 3.6 MeV with $S=0.33$. The largest possible experimental value in this region is $S_{5/2} \approx 0.03$. On the positive side Heyde *et al.* predict measurable $g_{9/2}$ strength at 2.4 and 2.9 MeV in fair agreement with some comparable $l=4$ strengths observed near 2.2 and 3.5 MeV.

We conclude that unified model calculations offer a good way to understand the extensive spreading of the single-particle strengths in ^{141}Ce . The improved resolution in this experiment has led to new values of S_j for a number of important states which agree even better with theory than those of Ref. 10. However, above 2 MeV in excitation energy the model space used seems to become increasingly inadequate as evidenced by a considerable underprediction of the number of levels observable in $^{140}\text{Ce}(d,p)$.

†Work supported by the National Science Foundation.

¹R. H. Fulmer, A. L. McCarthy, and B. L. Cohen, *Phys. Rev.* **128**, 1302 (1962).

²C. A. Wiedner, A. Heusler, J. Solf, and J. P. Wurm, *Nucl. Phys.* **A103**, 433 (1967).

³R. A. Brown and R. L. Mlekodaj, *Phys. Rev. C* **3**, 954 (1971).

⁴W. Gelletly, J. A. Moragues, M. A. Mariscotti, and W. R. Kane, *Phys. Rev. C* **1**, 1052 (1970).

⁵L. Lessard, S. Gales, and J. L. Foster, Jr., *Phys. Rev. C* **6**, 517 (1972).

⁶K. Pingel, Y. Ishizaki, J. Lokame, M. Koike, I. Nonaka, H. Ogata, and Y. Saji, *Inst. Nucl. Study, University of Tokyo Annual Report* (unpublished), Vol. 39, p. 1971.

⁷W. L. Talbert, Jr., J. W. Cook, and J. R. McConnell,

Nucl. Data Sheets **10** (1973).

⁸L. Veaser, J. Ellis, and W. Haeberli, *Phys. Rev. Lett.* **18**, 1063 (1967).

⁹R. L. Auble, *Nucl. Data Sheets* **10**, 151 (1973).

¹⁰W. Booth, S. Wilson, and S. S. Ipson, *Nucl. Phys.* **A238**, 301 (1975).

¹¹B. L. Cohen, J. B. Moorhead, and R. A. Moyer, *Phys. Rev.* **161**, 1257 (1967).

¹²W. W. Daehnick, *Phys. Rev.* **177**, 1763 (1969).

¹³M. J. Spisak, Ph.D. thesis, University of Pittsburgh, 1977 (unpublished).

¹⁴Calibration code SPIRO by J. Childs (unpublished).

¹⁵DWBA code and instructions written by P. D. Kunz (unpublished).

¹⁶J. D. Childs, W. W. Daehnick, and M. J. Spisak, *Phys. Rev. C* **10**, 217 (1974).

¹⁷F. D. Becchetti and G. W. Greenlees, Phys. Rev. 182, 1190 (1969).

¹⁸K. Heyde, M. Waroquier, and H. Vincx, Phys. Lett. 57B, 429 (1975); and private communication.

¹⁹W. Booth, S. Wilson, and S. S. Ipson, Nucl. Phys. A229, 61 (1974).

²⁰J. J. Kolata and W. W. Daehnick, Phys. Rev. C 5, 568 (1972).

²¹R. M. DelVecchio and W. W. Daehnick, Phys. Rev. C 6, 2095 (1972).

²²See also W. W. Daehnick and R. M. DelVecchio, Phys. Rev. C 11, 623 (1975).